Master of Science

Subretinal transplantation of human embryonic stem cell-derived retinal pigment epithelium (MA09-hRPE) : A safety and tolerability evaluation in minipigs

The Graduate School
of the University of Ulsan

Department of Medicine
Sung-Min Cho

Subretinal transplantation of human embryonic stem cell-derived retinal pigment epithelium (MA09-hRPE) : A safety and tolerability evaluation in minipigs

Supervisor : Woo-Chan Son

A Dissertation

Submitted to
the Graduate School of the University of Ulsan
In partial Fulfillment of the Requirements
for the Degree of

Master of Science

by

Sung-Min Cho

The Graduate School
of the University of Ulsan

Department of Medicine
August 2018

Subretinal transplantation of human embryonic stem cell-derived retinal pigment epithelium (MA09-hRPE) : A safety and tolerability evaluation in minipigs

This certifies that the master's thesis

of Sung-Min Cho is approved.

_____

Committee Chair Dr. Kyung-ja Cho

_____

Committee Member Dr. Joo Yong Lee

_____

Committee Member Dr. Woo-Chan Son

The Graduate School of the University of Ulsan

Department of Medicine

August 2018

Abstract

The transplantation of human embryonic stem cell (hESC)-derived retinal pigment epithelium (RPE) cells has been recently proposed as a therapy for age-related macular degeneration. This study aimed to determine the safety and tolerability of subretinal injection of hESC-derived RPE cells in the minipigs at a higher dose than the established clinical dose (5×10^4 cells/150 μL). The hESC-derived RPE cells (60 or 120×10^4 cells/150 μL) were injected under the retina of minipigs, and the animals were sacrificed at Weeks 4, 8, and 12 post-surgery. The treated eyes were examined by fundus photography, optical coherence tomography (OCT), histopathology, and fluorescence *in situ* hybridization (FISH). Bleb and pigmentation under the retina were observed by fundus photography and OCT immediately after injection and pigments on the retina appeared at Weeks 5, 9 and 12 after surgery. Microscopically, cell clusters consisted with uniform population of rounded or oval cells were seen on the RPE/choroid of injected eyes in all minipigs. Immunohistochemistry revealed that they were mostly T lymphocytes, and no fluorescence signals were detectable by FISH at the cell clusters of the treated eyes. Cell clusters were considered to be localized at the cell injection site; therefore, they could be caused by trauma of injection or cell volume. No other changes were observed. According to our data, it can be concluded that the subretinal injection of hESC-derived RPE cells (60 and 120×10^4 cells/150 μL) was considered safe for degenerative macular disease human trials.

Keywords: age-related macular degeneration, hESC-derived RPE cell, subretinal injection, preclinical study, minipig

Contents

List of Tables

List of Figures

Introduction

Dysfunction of the retinal pigment epithelium (RPE) has been observed in various retinal disorders such as age-related macular degeneration (AMD) which is the leading cause of irreversible blindness in people over 60 years of age [1]. The number of people with AMD will increase due to an increase in the ageing population [2]. Two subgroups of AMD are commonly distinguished: atrophic (dry form) and exudative (wet form). The dry form is typically characterized by a progressing course leading to degeneration of the RPE and photoreceptors [3]. The wet form is linked to choroidal neovascularization directed to the subretinal macular region [3]. Despite substantial progress in the development of new therapies for the wet form AMD included anti-VEGF medication injected into the eye or photodynamic therapy (PDT) [3], the severe visual disorder associated with geographic atrophy in the dry form AMD remains untreatable.

The RPE is a single layer of pigmented cells that reside at the back of the eye between the Bruch's membrane and the retina, which is essential for visual function. Recently, RPE replacement has been proposed as a novel therapeutic approach for dry form AMD. Preclinical tests for efficacy and safety analysis of RPE replacement were performed using well-established animal models of retinal degeneration [4, 5]. It was reported that transplanted cells could successfully integrate into a RPE monolayer using the Royal College of Surgeons (RCS) rat and Elov14 mouse [6]. Additionally, there was evidence that transplantation of hESC-derived RPE cells could maintain photoreceptors and prevent the loss of visual function [7-10].

A previous study reported the safety and potential efficacy of subretinal transplantation of hESC-derived RPE cells in four Asian patients [11]. The dose of transplanted cells was 5×10^4 cells/150 μL, and the patients were followed up for 1 year. There were no findings such as tumorigenesis, ectopic tissue formation, or other serious safety issues related to the transplanted cells. Furthermore, the improvement of visual functions was confirmed in the

previous study. We carried out our current study to determine the safety and tolerability of hESC-derived RPE cells following subretinal injection into minipigs at a higher dose than the established clinical dose of 5×10^4 cells/150 μL.

Pigs are often used in ophthalmological studies because the porcine eye has a similar vasculature to the human eye and has a comparable number and distribution of rod and cone cells [12]. Furthermore, the size of pig eye is anatomically similar to the size of the human eye [13, 14]. In principle, the animal model selected for preclinical toxicology studies should be normal and healthy with a low background incidence of pathological diseases and background lesions [15]. Therefore, in this study, we used healthy minipig animal models instead of disease animal models.

The injected doses were 60 and 120 $\times$ 10^4 RPE cells, and the treated animals were sacrificed at Weeks 4, 8, and 12 after this procedure. The treated eyes were monitored by fundus photography and optical coherence tomography (OCT) before necropsy. The harvested tissues were examined by routine histopathology, immunohistochemistry, and fluorescence in situ hybridization (FISH).

Materials and Methods

1. Study design

A total of 10 minipigs received subretinal xenografts of hESC-derived RPE (MA09-hRPE) cells. The first animal (Pig 1) was used to determine the design of the main study. The selected cell transplantation doses were 60 and 120 × 10^4 cells/150 μL on the basis of the preliminary study with 100 × 10^4 cells/150 μL. Each minipig was sacrificed at Weeks 4, 8, and 12 after injection. Balanced salt solution (BSS) instead of hESC-RPE cells was administered as a control in the eye of pig 10, and this animal was sacrificed after 12 weeks (Table 1).

Table 1. Study design.

Group	Dose (× 10^4 cells/150 μL)	Period under Observation	Animal No.
Pre	100	9 days	Pig 1
Control	0	12 weeks	Pig 10
Low	60	4 weeks	Pig 2
		4 weeks	Pig 6
		8 weeks	Pig 9
		12 weeks	Pig 7
High	120	4 weeks	Pig 3
		4 weeks	Pig 4
		8 weeks	Pig 8
		12 weeks	Pig 5

The administered doses of hESC-derived RPE cells were 60 and 120 × 10^4 cells/150 μL. Cells were injected under the retina of 10 minipigs and animals sacrificed at 4, 8, and 12 weeks after surgery.

2. Animal recipients

Laboratory minipigs (PWG genetics) that were 16 months old and weighed ~30 kg were

purchased from Medikinetics (Pyeongtaek, Korea) and the protocol was reviewed by Institutional Animal Care and Use Committee (IACUC) of Asan Medical Center and Ulsan University College of Medicine (IACUC No.: 2015-14-122).

The animals were individually housed in stainless steel cages measuring 152 × 92 × 102 cm and were fed once daily with a standard pig diet (Purinafeed, Seongnam, Korea). Drinking water purified by reverse osmosis was supplied through an automatic valve. Animal room controls were set to maintain a temperature and relative humidity of 22±2°C and 55±5%, respectively. The room was lit by fluorescent lighting to yield an artificial cycle of 12 h light/12 h dark.

The animals were treated with 2 mg/kg/day prednisolone (Solondo, Yuhan Corporation, Seoul, Korea) for immunosuppression from one week before the surgery to two weeks after surgery, and then were administered 1 mg/kg/day after two weeks.

3. Transplantation procedure and Post-surgical follow up

The transplantation procedure was performed by an ophthalmologist who subspecialized in retinal surgery. Prior to surgery, anesthesia was induced with intramuscular injection of xylazine (1 mg/kg; Rompun, Bayer), azaperon (2 mg/kg; stresnil, Janssen), and alfaxalone (2 mg/kg; Jurox), and was maintained with isoflurane gas under veterinary supervision. The surgical field was scrubbed with 10% povidone iodine and draped with a sterile field. An eyelid speculum was used to fix the eye of the minipig. The procedure was started using a 23-gauge trocar that was inserted at 60°, 120°, and 270° angles through the conjunctiva, and the trocar system was placed on the eye. BSS was a connected by cannula that supplied the fluid, and allowed for fluid flow into the vitreous cavity. After vitreous body removal, hESC-derived RPE cells were injected using a 38-gauge cannula into the subretinal space. Gentamicin (20 mg; Shinpoong, iansan, Korea) and dexamethasone (2.5 mg; Yuhan, Korea) were administered in the subconjunctival tissue to prevent infection and inflammation.

All animals were treated twice daily with 5 mg/kg cefazolin (Chong Kun Dang, Seoul,

Korea) by intramuscular injection for 48 h after surgery. The treated eyes were disinfected and bandaged twice daily for 4 weeks in order to protect the surgical site from physical impact or infection. Animals were inspected visually at least twice daily for evidence of ill-health or reactions to the treatment.

4. Fundus photography

After surgery, the treated eyes were confirmed using a fundus camera (hand-held retinal camera, Kowa, Tokyo, Japan). The fundus camera was used with mydriasis.

Before photography, anesthesia was induced using intramuscular injection of xylazine (1 mg/kg), azaperon (2 mg/kg), and alfaxalone (2 mg/kg), and was maintained with isoflurane gas. The minipig eye was fixed with an eyelid speculum, and measured in a dark environment. Photography was performed with the fundus camera at Day 1 and Week 1 after injection, and then at two-week intervals.

5. Optical coherence tomography

The minipig retinal layer was confirmed using optical coherence tomography (OCT, Carl Zeiss, Germany) that was developed for the noninvasive cross-sectional imaging of biological systems. OCT was performed at 24 h after injection and then once every two weeks.

Before photography, anesthesia was induced and maintained in the same manner as described for the fundus camera. OCT was also used with mydriasis using an eyelid speculum to keep the eye fixed.

6. Necropsy and histopathology

All animals were sacrificed at the end of each schedule by an intramuscular injection of xylazine and alfaxalone followed by exsanguination. Enucleated eyes were immediately fixed in Davidson's solution overnight at room temperature. Fixed eyes were dehydrated in

ethanol, cleared in xylene, and embedded in paraffin blocks. Sections of 3 μm thickness were cut and stained with hematoxylin and eosin (H&E).

7. Immunohistochemistry

Sections from paraffin-embedded tissue blocks of minipig eye tissues were cut at a 3 μm thickness and mounted on glass slides. Immunohistochemistry was carried out using a Benchmark XT (Ventana Medical Systems Inc., Tucson, AZ). Deparaffinization, epitope retrieval, and immunostaining were performed according to the manufacturer's instructions using cell conditioning solutions (CC1) and the BMK ultraView diaminobenzidine (DAB) detection system (Ventana Medical Systems). Slides were stained with anti-CD3 (ab828 and ab16669, Abcam, Cambridge, UK) and anti-CD45 (ab10558, Abcam). Positive signals were amplified using ultraView copper, and sections were counterstained with hematoxylin and bluing reagent. Pig 6 (60×10^4 cells/150 μL, 4 weeks post-injection) sample was examined by immunohistochemistry, and minipig lymph nodes were used as a positive control.

8. Fluorescence *in situ* hybridization (FISH)

FISH specimen was the injected eye of pig 9 (60×10^4 cells/150 μL, 8 weeks post-injection). The samples for the study were routinely formalin-fixed, paraffin-embedded (FFPE) tissue preparations. FFPE tissue blocks were cut on a microtome into serial 3 μm sections. A DNA probe kit (Vysis CEP X SpectrumOrange/ Y SpectrumGreen) was obtained from Abbott. FISH staining of FFPE sections was performed by FISH automation with a VP 2000 processor. After the staining procedure, slides were scanned using a Zeiss LSM 710 microscope to obtain fluorescence signals from the samples. CEP X SpectrumOrange probe fluorescence was detected with Rhod-2 filter (577nm), and CEP Y SpectrumGreen probe was detected using Adirondack Green 520 filter (520nm). DAPI was detected using a standard DAPI filter (465nm).

Results

1. Fundus photography

Retinal images of each animal were obtained using a fundus camera, and subretinal blebs and pigmentation were observed in fundus oculi of the treated eyes.

Subretinal blebs caused by transplantation of hESC-derived RPE cells were formed at Day 1 after surgery (Fig. 1A). The presence of these blebs was also confirmed at Week 1 (Fig. 1B), but they had disappeared at Week 3 after subretinal injection (Fig. 1C). The border of the injected cells was sharp at Day 1 after surgery, but changed indistinctly at Week 1 (Fig 1A, 1B, yellow arrows). This phenomenon suggested that the injected cells were absorbed. Subretinal pigmentation appeared at Week 5 after transplantation at the site where the blebs were present (Fig. 1D, green arrow), and epiretinal pigmentations were observed at Weeks 9 and 12 after surgery (Fig. 1E, 1F, white arrows). No abnormalities of the ocular vasculature due to transplantation were evident on the fundus photographs, and no findings such as fibrosis and mineralization were also confirmed during the period under observation (Fig. 1A-F).

2. Optical coherence tomography

OCT was performed to identify the influence of hESC-derived RPE cells injection on the retinal layer. It was confirmed that the transplanted cells were properly injected in the subretinal space.

Subretinal blebs appeared in the treated eyes immediately after transplantation (Fig. 2A-B, 2E-F), but were no longer observed at Day 14 post-surgery (Fig. 2C-D, 2G-H).

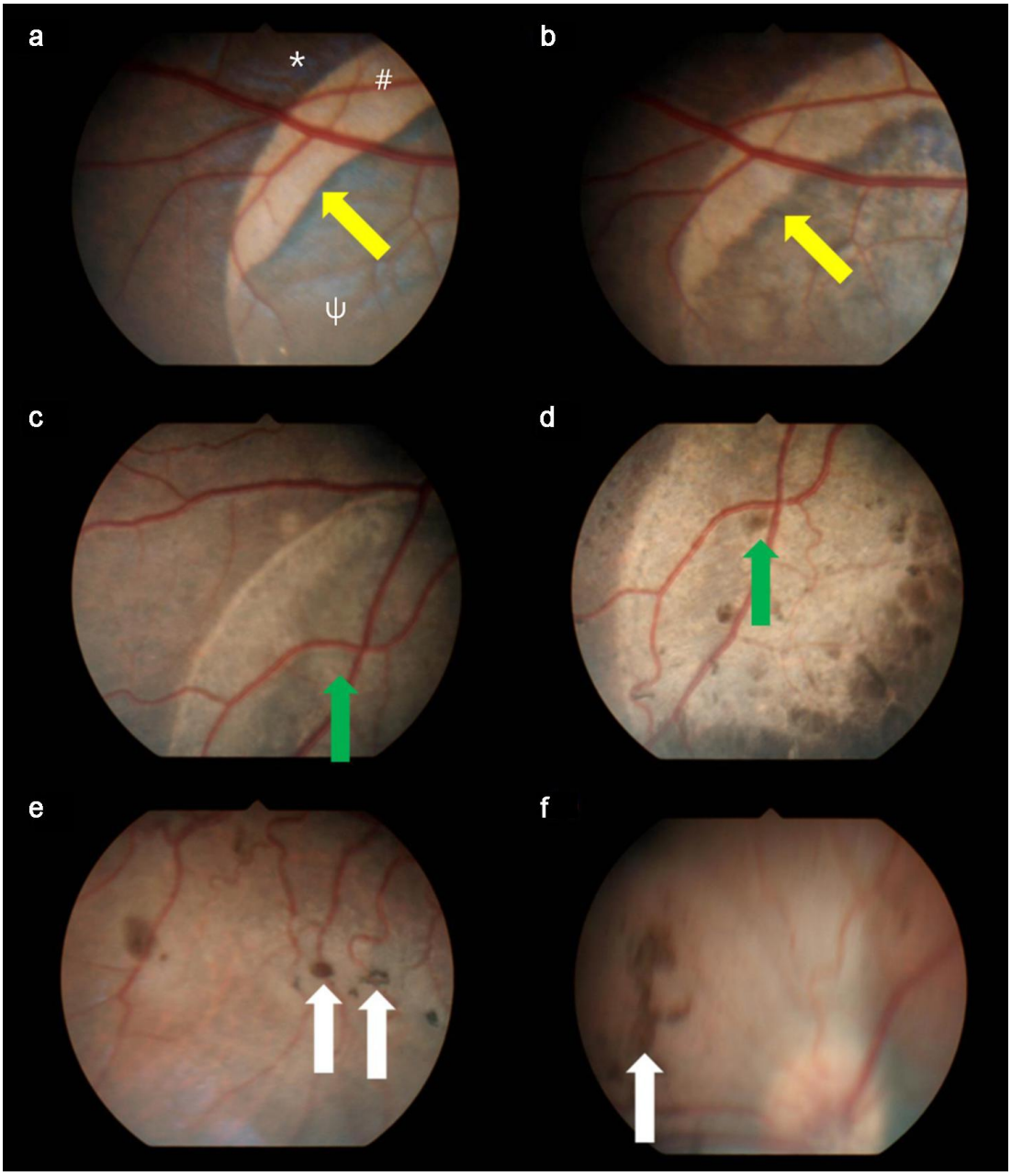

Figure 1. Representative fundus photographs of treated eyes. Fundus photographs were at (A) Day 1, (B) Week 1, (C) Week 3, (D) Week 5, (E) Week 9, and (F) Week 12 after subretinal injection. A subretinal bleb (the pale semicircle) was observed at Day 1 and Week 1 after injection (A, B), but disappeared at Week 3 post-surgery (C). Yellow arrows indicate the alteration of the border of in injected cells, and this means that the injected cells were being absorbed. Green arrows show that new subretinal pigment appeared (C, D). Pigments on the retina were also observed at Weeks 9 and 12 post-injection (E, F). White arrows

indicate individual pigments formed on the retina. Other findings were absent. (*: normal fundus, #: formed bleb, ψ : injected cell cluster)

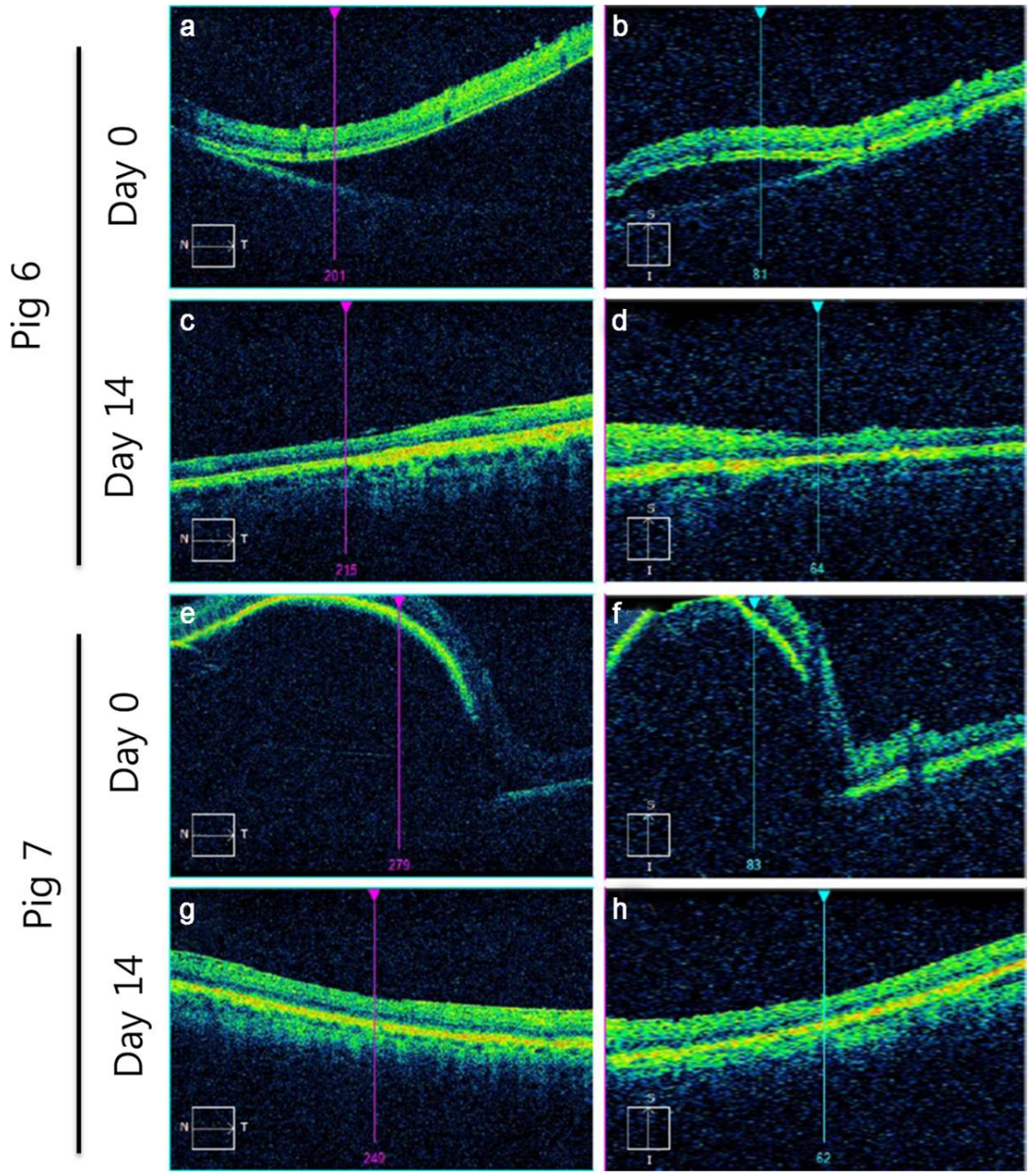

Figure 2. Representative OCT images from the treated eyes of pig 6 (A-D) and 7 (E-H). (A), (B), (E) and (F) were taken at Day 0 and (C), (D), (G) and (F) were taken at Day 14 after surgery. Subretinal blebs were observed immediately after transplantation, but were reduced at Day 14 after surgery. No other specific structural changes were evident.

3. Histopathology

Minipig eyes were examined histologically, and cell clusters were observed at the RPE/choroid in all of the injected eyes (Fig. 3). These cell clusters were located between the sclera and retina, and were composed of a uniform population of cells having rounded or oval nuclei with little cytoplasm.

The cell cluster sizes differed depending on the transplantation dose and period under observation. As the dose increased and observation period decreased, the size of the cell cluster increased (Fig. 3A–F). Cell clusters were not detected in the control animal (Fig. 4).

No abnormality of anatomical ocular structure, such as compression of the adjacent tissue, was observed. There was no evidence of abnormal proliferation, tumorigenesis, or other adverse findings due to transplantation of hESC-derived RPE cells.

4. Immunohistochemistry

To identify the cell cluster observed in the H&E stained sections, we performed immunohistochemistry using anti-CD3, anti-CD45 and anti-cytokeratin7 antibodies.

Specific membranous or cytoplasmic positive staining was seen with both CD45 (Fig. 5C) and CD3 (Fig. 5D, 5E) antibodies in majority of the cells in the clusters of treated eyes but not in those of untreated eyes. Furthermore, the cell cluster of the injected eye was cytokeratin7-negative (Fig. 6).

Both CD3 and CD45 are T lymphocyte specific marker; therefore, the cell cluster was composed of mostly T lymphocytes.

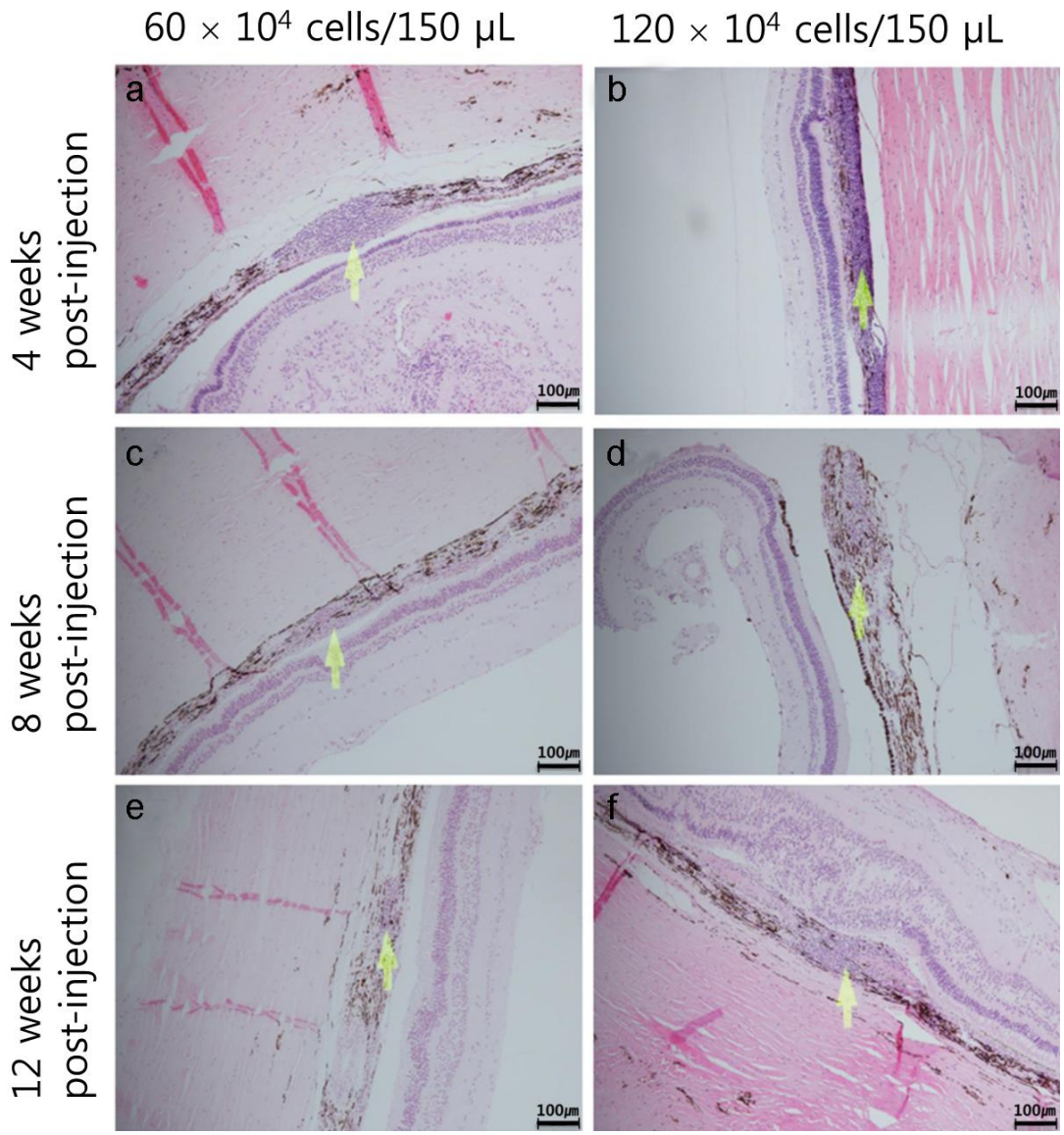

Figure 3. Representative microscopic images of pig retinas stained with H&E (×100). Yellow arrows indicate individual cell clusters. Larger cell cluster sizes were observed depending on increase of the dose (A-C-E/B-D-F), and decrease of period under observation (A-B/C-D/E-F).

(A) Pig 2, 60×10^4 cells/150 μL, 4 weeks post-injection.

(B) Pig 3, 120×10^4 cells/150 μL, 4 weeks post-injection.

(C) Pig 9, 60×10^4 cells/150 μL, 8 weeks post-injection.

(D) Pig 8, 120×10^4 cells/150 μL, 8 weeks post-injection.

(E) Pig 7, 60×10^4 cells/150 μL, 12 weeks post-injection.

(F) Pig 5, 120×10^4 cells/150 μL, 12 weeks post-injection.

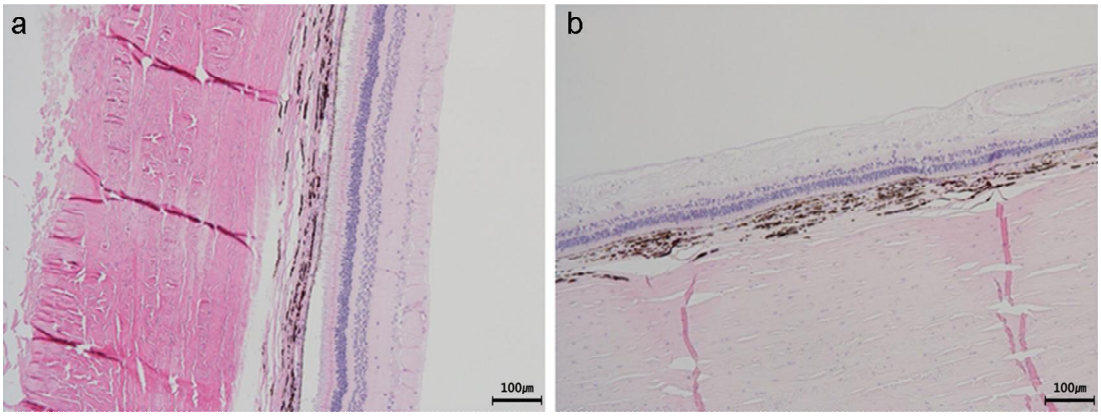

Figure 4. Negative control retinas stained with H&E. (A) The injected eye of pig 10. (B) The non-injected eye of pig 1. No cell clusters, inflammation, or fibrosis caused by surgery were confirmed in control slides.

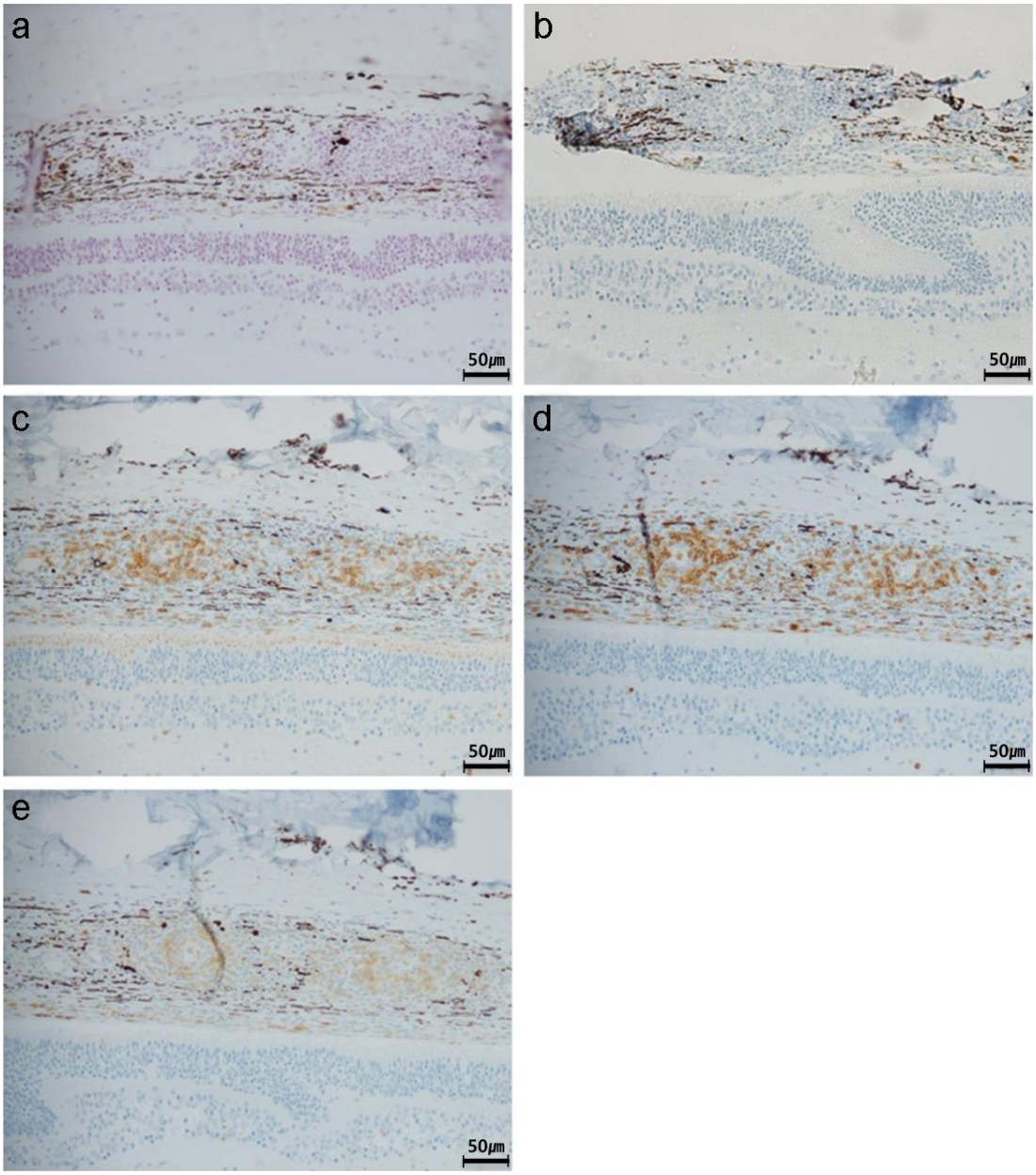

Figure 5. Immunohistochemical analyses of treated pig retinas (×200). Sections were stained with (A) H&E, (B) buffer negative control (no primary antibody), (C) anti-CD45 antibody, (D) or (E) anti-CD3 antibody. The surrounding ocular tissue and RPE layer without cell cluster were CD3- and CD45-negative, and rounded or oval cells located in the cell clusters were stained by anti-CD3 and anti-CD45 antibodies.

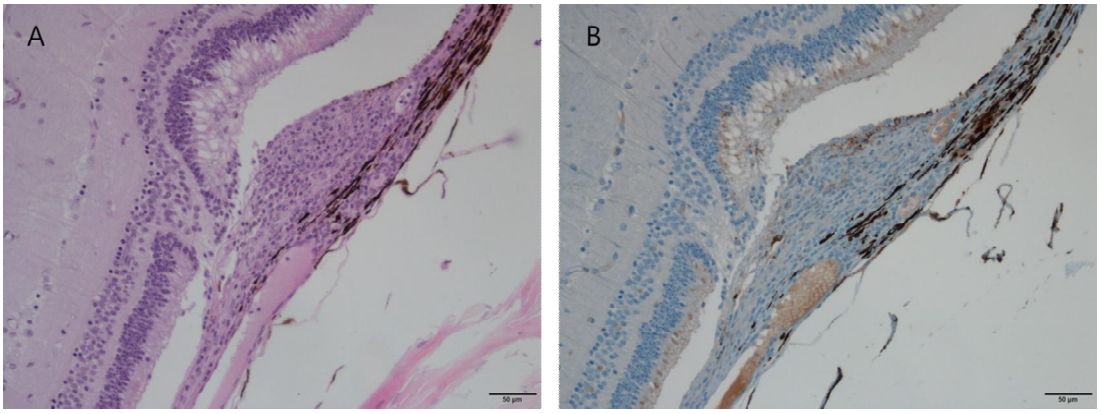

Figure 6. Immunohistochemical analyses using anti-cytokeratin7 antibody (x200). Sections were stained with (A) H&E and (B) anti-cytokeratin7 antibody. The cell cluster was cytokeratin7-negative.

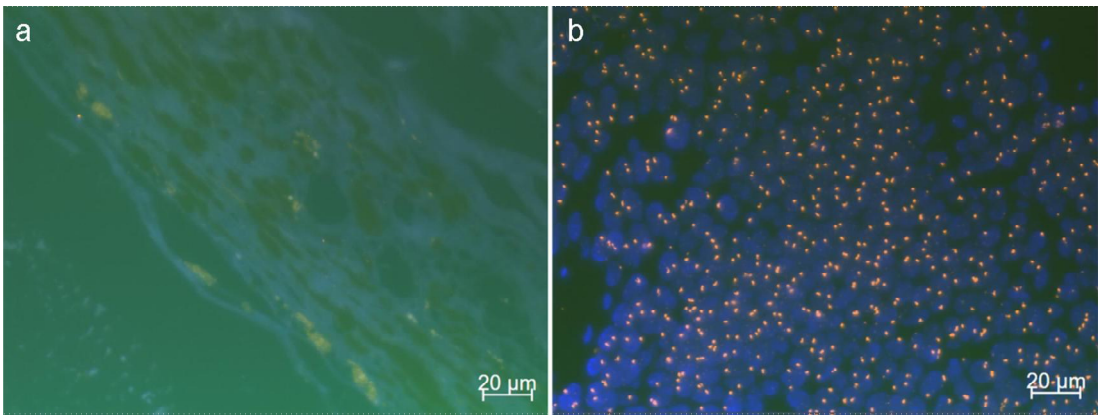

Figure 7. Representative FISH images. (A) The treated eye tissue of pig 9 (60×10^4 cells/150 μL, 8 weeks post-injection) and (B) positive control cells. Fluorescent images were captured using Rhod-2 filter, Adirondack Green 520 filter, and DAPI filter. (A) No fluorescence signals were detectable in the cell clusters that had been observed previously by H&E staining. (B) Orange fluorescence signals appeared to be significant in the nuclei of the positive-control cells.

5. Fluorescence *in situ* hybridization (FISH)

FISH was used to determine the presence of injected cells with the DNA probe of Vysis CEP X SpectrumOrange/Y SpectrumGreen.

In the FISH assay, no fluorescence signals were detectable in the cell clusters in the slides of treated minipig eyes (Fig 7A). The ocular tissue was stained blue by DAPI, and orange and green fluorescence signals were undetected.

A hESC-derived RPE cell block was used as a positive control. Orange staining of the X chromosomes in the nuclei of cells appeared to be marked, and cells stained with DAPI were clearly observed in the positive control slide (Fig 7B).

Discussion

This present study provides an evaluation of the safety and tolerability of subretinal injection of hESC-derived RPE cells (MA09-RPE cells) in a minipig model at higher dose than that used in clinical trials. Fundus photography and OCT were used to monitor the treated eyes during the study periods, and histopathological examination and FISH were conducted using eyeball samples. The fundus camera and OCT observations revealed the appearance of a bleb immediately after surgery, which disappeared after 3 weeks. The injected cells under the retina could be observed by fundus camera, and the area of these cells shrank at Week 1 after transplantation, because a part of the injected cells was absorbed from Day 1 to Week 1 after the procedure. Pigments on the retina were formed at Week 5 after transplantation, and also appeared at Weeks 9 and 12 after surgery. These findings were thought to be due to the normal proliferation of unabsorbed cells.

In the histological examinations, cell clusters composed of a uniform population of CD3- and CD45-positive cells having rounded or oval nucleus with little cytoplasm appeared in the RPE/choroid without evidence of tumorigenesis. As the dose increase and observation period decrease, these cell cluster sizes increased. The cell clusters were considered to be localized at the cell injection site and therefore these were most likely caused by trauma of injection or cell volume. According to Sinha's paper, the incidence of mononuclear cell infiltrate in the choroid and the ciliary body of untreated cynomolgus monkeys was seen in approximately 25% of drug safety evaluation studies; additionally, the microscopically observed mononuclear cell infiltrate in the choroid and ciliary body appears to not be associated with any obvious disease process or functional deficit [16]. Thus, it was considered that the cell clusters observed in our study were not serious adverse events.

Vysis CEP X SpectrumOrange/Y SpectrumGreen DNA probes were used to detect specific gene sequences on defined regions of the X and Y chromosomes. According to the article associated with the FISH probe, FISH images of male cells showed only the expected

Orange X and Green Y signals, whereas FISH images of female cells had only two orange X labels in each of the scanned cells [17]. Since the injected cells were female origin, it was expected that the injected cells have orange fluorescence signals. In our current study, orange fluorescence signals could be detected in the positive control, while they were not detected in the cell clusters of the treated eyes. Because it was difficult for all parts of the ocular tissue to be examined by FISH, it was uncertain whether there were any injected cells present in the entire treated ocular tissue. Furthermore, the presence of transplanted cells was confirmed in a comparable study [18].

Tumor formation is one of the major limitations for use of stem cells in therapeutic applications [19-21]. For this reason, tumorigenesis is identified for safety of stem cells in many studies [22, 23]. The transplantation of undifferentiated stem cells is known to be associated with teratoma formation, and this complication was recently reported after the subretinal transplantation of mouse ESC-derived neural cells [24]. Human ESC-derived RPE cells have been studied over a long period and been found to exhibit sustained function without evidence of teratoma formation [4]. In our current study, there was no evidence of tumorigenesis in the treated eyes.

OCT has been used to visualize retinal layers and has allowed researchers to identify microstructural alterations continuously during the trial period. It has been reported that in mice, degenerative diseases of the retina can be observed by OCT [25]. Moreover, microstructural alterations in the atrophic region such as outer retinal tubulations, irregular elevations of the RPE/Bruch membrane complex, crown-like elevations with underlying debris, and plaques in the outer retinal layer have been confirmed by OCT [26]. It was also reported that retinal detachment, subretinal fibrosis, and atrophy were diagnosed by OCT [27-29]. Herein, we used this technique to confirm retinal alterations, and only the induced bleb was observed immediately after surgery. No other alterations such as fibrosis, or atrophy were evident in this analysis.

In conclusion, it was seen that subretinal transplantation of high dose hESC-derived RPE

cells was well tolerated in a preclinical trial using minipigs. Our current data suggest that 60 and 120 $\times$ 10^4 cells/150 μL of hESC-derived RPE cells could be used for degenerative macular disease human trials.

References

1. Pascolini D, Mariotti SP, Pokharel GP, Pararajasegaram R, Etya'ale D, Negrel AD, et al. 2002 global update of available data on visual impairment: a compilation of population-based prevalence studies. Ophthalmic Epidemiol. 2004;11:67-115.
2. Friedman DS, O'Colmain BJ, Munoz B, Tomany SC, McCarty C, de Jong PT, et al. Prevalence of age-related macular degeneration in the United States. Archives of ophthalmology (Chicago, Ill : 1960). 2004;122:564-72. http://doi.org/10.1001/archopht.122.4.564.
3. Nowak JZ. Age-related macular degeneration (AMD): pathogenesis and therapy. Pharmacological reports : PR. 2006;58:353-63.
4. Lu B, Malcuit C, Wang S, Girman S, Francis P, Lemieux L, et al. Long-term safety and function of RPE from human embryonic stem cells in preclinical models of macular degeneration. Stem cells (Dayton, Ohio). 2009;27:2126-35. http://doi.org/10.1002/stem.149.
5. da Cruz L, Chen FK, Ahmado A, Greenwood J, Coffey P. RPE transplantation and its role in retinal disease. Progress in retinal and eye research. 2007;26:598-635. http://doi.org/10.1016/j.preteyeres.2007.07.001.
6. Schwartz SD, Tan G, Hosseini H, Nagiel A. Subretinal Transplantation of Embryonic Stem Cell-Derived Retinal Pigment Epithelium for the Treatment of Macular Degeneration: An Assessment at 4 Years. Investigative ophthalmology & visual science. 2016;57:ORSFc1-9. http://doi.org/10.1167/iovs.15-18681.
7. Lund RD, Wang S, Klimanskaya I, Holmes T, Ramos-Kelsey R, Lu B, et al. Human embryonic stem cell-derived cells rescue visual function in dystrophic RCS rats. Cloning and stem cells. 2006;8:189-99.

http://doi.org/10.1089/clo.2006.8.189.

8. Plaza Reyes A, Petrus-Reurer S, Antonsson L, Stenfelt S, Bartuma H, Panula S, et al. Xeno-Free and Defined Human Embryonic Stem Cell-Derived Retinal Pigment Epithelial Cells Functionally Integrate in a Large-Eyed Preclinical Model. Stem cell reports. 2016;6:9-17. http://doi.org/10.1016/j.stemcr.2015.11.008.

9. Carido M, Zhu Y, Postel K, Benkner B, Cimalla P, Karl MO, et al. Characterization of a mouse model with complete RPE loss and its use for RPE cell transplantation. Investigative ophthalmology & visual science. 2014;55:5431-44. http://doi.org/10.1167/iovs.14-14325.

10. Li Y, Tsai YT, Hsu CW, Erol D, Yang J, Wu WH, et al. Long-term safety and efficacy of human-induced pluripotent stem cell (iPS) grafts in a preclinical model of retinitis pigmentosa. Molecular medicine (Cambridge, Mass). 2012;18:1312-9. http://doi.org/10.2119/molmed.2012.00242.

11. Song WK, Park KM, Kim HJ, Lee JH, Choi J, Chong SY, et al. Treatment of macular degeneration using embryonic stem cell-derived retinal pigment epithelium: preliminary results in Asian patients. Stem cell reports. 2015;4:860-72. http://doi.org/10.1016/j.stemcr.2015.04.005.

12. Chader GJ. Animal models in research on retinal degenerations: past progress and future hope. Vision research. 2002;42:393-9.

13. He YG, McCulley JP, Alizadeh H, Pidherney M, Mellon J, Ubelaker JE, et al. A pig model of Acanthamoeba keratitis: transmission via contaminated contact lenses. Investigative ophthalmology & visual science. 1992;33:126-33.

14. Danis RP, Bingaman DP. Insulin-like growth factor-1 retinal microangiopathy in the pig eye. Ophthalmology. 1997;104:1661-9.

15. Dixit R, Boelsterli UA. Healthy animals and animal models of human

disease(s) in safety assessment of human pharmaceuticals, including therapeutic antibodies. Drug discovery today. 2007;12:336-42. http://doi.org/10.1016/j.drudis.2007.02.018.

16. Sinha DP, Cartwright ME, Johnson RC. Incidental mononuclear cell infiltrate in the uvea of cynomolgus monkeys. Toxicologic pathology. 2006;34:148-51. http://doi.org/10.1080/01926230500531779.

17. Dziegelewski M, Simich JP, Rittenhouse-Olson K. Use of a Y chromosome probe as an aid in the forensic proof of sexual assault. Journal of forensic sciences. 2002;47:601-4.

18. Shim SH, Kim G, Lee DR, Lee JE, Kwon HJ, Song WK. Survival of Transplanted Human Embryonic Stem Cell-Derived Retinal Pigment Epithelial Cells in a Human Recipient for 22 Months. JAMA ophthalmology. 2017;135:287-90. http://doi.org/10.1001/jamaophthalmol.2016.5824.

19. Stadtfeld M, Nagaya M, Utikal J, Weir G, Hochedlinger K. Induced pluripotent stem cells generated without viral integration. Science (New York, NY). 2008;322:945-9. http://doi.org/10.1126/science.1162494.

20. Kaji K, Norrby K, Paca A, Mileikovsky M, Mohseni P, Woltjen K. Virus-free induction of pluripotency and subsequent excision of reprogramming factors. Nature. 2009;458:771-5. http://doi.org/10.1038/nature07864.

21. Okita K, Hong H, Takahashi K, Yamanaka S. Generation of mouse-induced pluripotent stem cells with plasmid vectors. Nature protocols. 2010;5:418-28. http://doi.org/10.1038/nprot.2009.231.

22. Kokkinaki M, Sahibzada N, Golestaneh N. Human induced pluripotent stem-derived retinal pigment epithelium (RPE) cells exhibit ion transport, membrane potential, polarized vascular endothelial growth factor secretion, and gene expression pattern similar to native RPE. Stem cells (Dayton, Ohio). 2011;29:825-35. http://doi.org/10.1002/stem.635.

23. Idelson M, Alper R, Obolensky A, Ben-Shushan E, Hemo I, Yachimovich-Cohen N, et al. Directed differentiation of human embryonic stem cells into functional retinal pigment epithelium cells. Cell stem cell. 2009;5:396-408. http://doi.org/10.1016/j.stem.2009.07.002.

24. Arnhold S, Klein H, Semkova I, Addicks K, Schraermeyer U. Neurally selected embryonic stem cells induce tumor formation after long-term survival following engraftment into the subretinal space. Investigative ophthalmology & visual science. 2004;45:4251-5. http://doi.org/10.1167/iovs.03-1108.

25. Li Q, Timmers AM, Hunter K, Gonzalez-Pola C, Lewin AS, Reitze DH, et al. Noninvasive imaging by optical coherence tomography to monitor retinal degeneration in the mouse. Investigative ophthalmology & visual science. 2001;42:2981-9.

26. Moussa K, Lee JY, Stinnett SS, Jaffe GJ. Spectral domain optical coherence tomography-determined morphologic predictors of age-related macular degeneration-associated geographic atrophy progression. Retina (Philadelphia, Pa). 2013;33:1590-9. http://doi.org/10.1097/IAE.0b013e31828d6052.

27. Fleckenstein M, Charbel Issa P, Helb HM, Schmitz-Valckenberg S, Finger RP, Scholl HP, et al. High-resolution spectral domain-OCT imaging in geographic atrophy associated with age-related macular degeneration. Investigative ophthalmology & visual science. 2008;49:4137-44. http://doi.org/10.1167/iovs.08-1967.

28. Wolfensberger TJ, Gonvers M. Optical coherence tomography in the evaluation of incomplete visual acuity recovery after macula-off retinal detachments. Graefe's archive for clinical and experimental ophthalmology = Albrecht von Graefes Archiv fur klinische und experimentelle Ophthalmologie. 2002;240:85-9.

29. Souied EH, Miere A, Cohen SY, Semoun O, Querques G. Optical Coherence Tomography Angiography of Fibrosis in Age-Related Macular Degeneration. Developments in ophthalmology. 2016;56:86-90. http://doi.org/10.1159/000442783.

Summary in Korean

최근에는 연령관련 황반변성 치료를 목적으로 사람 배아 줄기세포에서 유래한 망막색소 상피세포 이식이 사용되고 있다. 본 시험에서는 사람 배아 줄기세포에서 유래한 색소 상피세포를 임상치료에서 설정된 용량(5×10^4 cells/150 μL)보다 더 높은 용량으로 미니피그에 망막하 주사하여 이에 대한 안전성을 확인하기 위해 수행하였다.

사람 배아 줄기세포에서 유래한 망막 색소 상피세포 60×10^4 cells/150 μL 또는 120×10^4 cells/150 μL 를 미니피그 망막하에 주사하고 수술 후 4, 8, 12 주 후에 부검하였다. 이식한 눈은 안저카메라, 빛간섭단층촬영, 조직병리학적 검사, 형광동소혼성화를 이용하여 검사하였다.

안저카메라와 빛간섭단층촬영을 통해 블랩과 망막의 색소침착을 관찰하였고, 이는 투여 후 5 주부터 감소하였다. 현미경 상에서 구형의 단일세포로 구성된 세포 무리가 모든 투여한 눈의 망막색소상피/맥락막에서 관찰되었다. 면역조직화학을 통해 세포 무리가 대부분 T 림프구로 구성되어 있다는 것을 확인하였고, 형광동소혼성화를 통해 투여된 세포가 남아 있지 않다는 것을 확인하였다. 세포 무리는 세포를 주사한 곳에 위치한 것으로 보이므로 세포 무리는 주사와 세포 부피에 의한 트라우마가 원인일 수 있다. 세포 무리 외에 괴사, 자가세포사멸, 광물화, 종양형성과 같은 변화는 관찰되지 않았다.

결론적으로 망막변성질환 치료를 위해 사람 배아 줄기세포에서 유래한 망막 색소상피세포 60×10^4 cells/150 μL 와 120×10^4 cells/150 μL 를 투여하는 것은 안전한 것으로 판단된다.